1521-009X/43/11/1702–1710$25.00
Drug Metabolism and Disposition

http://dx.doi.org/10.1124/dmd.115.064881
Drug Metab Dispos 43:1702–1710, November 2015

Combined Contribution of Increased Intestinal Permeability and Inhibited Deglycosylation of Ginsenoside Rb1 in the Intestinal Tract to the Enhancement of Ginsenoside Rb1 Exposure in Diabetic Rats after Oral Administration

Can Liu, Mengyue Hu, Haifang Guo, Mian Zhang, Ji Zhang, Feng Li, Zeyu Zhong, Yang Chen, Ying Li, Ping Xu, Jia Li, Li Liu, and Xiaodong Liu

Center of Drug Metabolism and Pharmacokinetics, China Pharmaceutical University, Nanjing, China (C.L., M.H., M.Z., J.Z., F.L., Z.Z., Y.C., Y.L., P.X., J.L., L.L., X.L.); Department of Biochemistry and Molecular Biology, Miller School of Medicine, University of Miami, Miami, Florida (C.L.); and Bioanalytical and Pharmacokinetics/Toxicokinetics Center, Jiangsu Tripod Preclinical Research Laboratories Inc., Nanjing, China (H.G.)

Received April 18, 2015; accepted August 10, 2015

ABSTRACT

Panax ginseng is becoming a promising antidiabetic herbal medication. As the main active constituents of Panax ginseng, ginsenosides are well known, poorly absorbed chemicals. However, the pharmacokinetic behavior of ginsenosides under diabetic conditions is not fully understood. This study aimed to explore the alterations and potential mechanisms of pharmacokinetic behavior of ginsenoside Rb1 in diabetic rats compared with normal rats and rats fed a high-fat diet. Systemic exposure (area under the concentration-time curve extrapolated from zero to infinity) was significantly increased in diabetic rats after oral administration of Rb1. Oral bioavailability of Rb1 was significantly higher in diabetic rats (2.25%) compared with normal rats (0.90%) and rats fed a high-fat diet (0.78%). Further studies revealed that increased Rb1 exposure in diabetic rats may be mainly attributed to increased Rb1 absorption via the intestine and inhibited Rb1 deglycosylation by the intestinal microflora. Neither metabolic enzymes nor drug transporters displayed appreciable effects on Rb1 disposition. The transport of paracellular markers (fluorescein sodium and fluorescein isothiocyanate-dextran of 4 kDa) as well as Rb1 itself across the Caco-2 monolayer cultured with diabetic serum was promoted, demonstrating that increased paracellular permeability of the Caco-2 monolayer may benefit intestinal Rb1 absorption. In addition, Rb1 exposure was decreased in diabetic rats after Rb1 intravenous administration, which may result from increased Rb1 urinary excretion. In conclusion, Rb1 oral exposure was significantly increased under diabetic conditions, which is of positive significance to clinical treatment. The potential mechanism may be associated with the combined contribution of increased gut permeability and inhibited deglycosylation of ginsenoside Rb1 by intestinal microflora.

Introduction

Panax ginseng (*Panax ginseng* C.A. Meyer) is becoming a popular remedy and dietary supplement, and it has a broad range of pharmacologic actions (Attele et al., 1999). Ginsenosides are considered to be the main effective constituents of Panax ginseng, among which ginsenoside Rb1 is one of the most abundant components. Accumulating evidence has shown that ginsenosides, including Rb1, possess antidiabetic properties (Kimura et al., 1981; Sotaniemi et al., 1995; Vuksan et al., 2000; Attele et al., 2002; Xie et al., 2005; Liu et al., 2014). However, oral bioavailability of Rb1, Rg1, and Rh2 was reported to be only 0.1%, 2%, and 5%, respectively (Odani et al., 1983a,b). As a result, it remains to be clarified how low plasma concentrations of ginsenosides exert glucose-lowering action.

Accumulating reports demonstrate that diabetes may influence the pharmacokinetics of numerous drugs. For example, faster clearance and a lower area under the concentration-time curve (AUC) of telithromycin and clarithromycin were shown in diabetic rats (Kim et al., 2005; Lee and Lee, 2008). In another study, diabetes induced increased the plasma concentration of verapamil after oral administration (Hu et al., 2011). Diabetes not only affects protein, lipid, and carbohydrate metabolism, but it also regulates metabolic enzymes and transporters as well as gastric emptying, nonenzymatic glycation of albumin, and renal function, all of which are involved in drug pharmacokinetics (Dostalek et al., 2012). Alterations of activity and expression of cytochrome P450 (P450) enzymes and drug transporters by diabetes were mostly considered as the potential underlying mechanism. We previously

This research was supported by the National Youth Science Foundation of China [Grant 81102503], the Fundamental Research Funds for the Central Universities [Grant JKY2011018], and the National Science Foundation of China [Grant 81273587].

dx.doi.org/10.1124/dmd.115.064881.

ABBREVIATIONS: AUC, area under the concentration-time curve; C-K, compound K; DMEM, Dulbecco's modified Eagle's medium; FD4, fluorescein isothiocyanate-dextran of 4 kDa; FLU, fluorescein sodium; HBSS, Hanks' balanced salt solution; HFD, high-fat diet; LC-MS, liquid chromatography–mass spectrometry; MDR1-MDCK, Multi-drug resistance protein 1 over-expressed MDCK cells; Oatp, organic anion-transporting polypeptide; P450, cytochrome P450; P-gp, P-glycoprotein; PPD, protopanaxadiol; SGLT1, sodium-dependent glucose transporter 1; STZ, streptozotocin; TEER, transepithelial electrical resistance.

reported that diabetes oppositely altered pharmacokinetic behaviors of verapamil after oral and intravenous administration to rats via oppositely regulating the activity and expression of hepatic and intestinal CYP3A, respectively (Hu et al., 2011). The exposure of orally administered glibenclamide induced by diabetes was increased, which attributed to both impaired hepatic CYP2C11 and intestinal breast cancer resistance protein activity and expression (Liu et al., 2012). Similarly, exposure of berberine after oral dosing was increased in diabetic rats due to downregulated intestinal P-glycoprotein (P-gp) (Yu et al., 2010). In addition, intestinal mucosa with intact tight junctions also serves as a main barrier to the passage of some drugs. For most of the ginsenosides, a large molecular mass (>500 Da), high hydrogen bond counts, and high molecular flexibility were responsible for their low membrane permeability (Liu et al., 2009). Previous studies showed that patients with diabetes displayed high serum zonulin levels, which were associated with increased intestinal permeability (Bosi et al., 2006; Sapone et al., 2006). These findings indicated that pharmacokinetic behaviors of ginsenosides may be greatly changed on account of the alteration of P450s, transporters, or intestinal permeability under diabetic conditions.

It is generally accepted that ginsenosides are extensively degraded by intestinal microflora in the gastrointestinal tract (Hasegawa et al., 1996; Tawab et al., 2003; Liu et al., 2009). Rb1, belonging to 20-(*S*)-protopanaxadiol (PPD)–type saponins (Fig. 1A), can be transformed to ginsenoside Rd, ginsenoside Rg3, ginsenoside F2, ginsenoside Rh2, compound K (C-K), and 20-(*S*)-PPD via stepwise cleavage of four sugar moieties at the C-3 and C-20 positions (Fig. 1B). Disorder of the intestinal microflora was verified under diabetic conditions, indicating that the alterations of biotransformation catalyzed by the intestinal microflora may affect degradation of ginsenosides in the intestinal gut, leading to changed pharmacokinetic properties of ginsenosides.

This study was designed to investigate whether the pharmacokinetic profiles of Rb1 were altered in rats with type 2 diabetes induced by a combination of a high-fat diet (HFD) and low-dose streptozotocin (STZ). Possible influential factors, including alteration of P450 enzymes, transporters, gut permeability, and deglycosylation metabolism induced by diabetes, were taken into consideration. Because of its potential as a therapeutic agent for diabetes, a comprehensive study on the pharmacokinetic characteristics of Rb1 under diabetic conditions is definitely worthwhile.

Materials and Methods

Chemicals. Ginsenosides Rb1, Rd, Rg3, F2, and Rh2 as well as C-K and 20-(*S*)-PPD (purity >99%) were purchased from Jilin University (Changchun, China). Pentobarbital, digoxin, STZ, verapamil, cyclosporine A, bromosulfalein, rifampicin, naringin, levofloxacin, fluorescein isothiocyanate-dextran of 4 kDa (FD-4), and fluorescein sodium (FLU) were obtained from Sigma-Aldrich (St. Louis, MO). High-performance liquid chromatography–grade methanol and acetonitrile were obtained from Merck (Darmstadt, Germany). All other reagents were of analytical grade and were commercially available.

Animals. Male Sprague-Dawley rats (weighing 100–120 g) were purchased from Sino-British Sipper and BK Laboratory Animal Ltd. (Shanghai, China) and acclimated to the laboratory environment for 3 days. The rats were maintained in a controlled environment (23°C ± 1°C temperature and 50% ± 5% relative humidity) with a 12-hour light/dark cycle. Water and food were provided ad libitum. All animal studies were conducted according to protocols approved by the Animal Ethics Committee of China Pharmaceutical University.

Induction of Diabetic Rats. Diabetic rats were induced as described previously by a combination of HFD and low-dose STZ injection (Chen et al., 2011, Liu et al., 2013). Briefly, rats were randomly divided into three groups: control rats, HFD-fed rats, and diabetic rats. Control rats were fed normal chow, whereas both HFD-fed rats and diabetic rats were fed a HFD (Xietong Biotech, Jiangsu, China) that consisted of 15% lard, 5% sesame oil, 20% sucrose, 2.5% cholesterol, and 57.5% normal chow. After 4 weeks of dietary manipulation, diabetic rats received an intraperitoneal injection of STZ (35 mg/kg, dissolved in citrate buffer, pH 4.5). Both HFD and control rats received only citrate buffer. Subsequently, the experimental rats maintained their original diets. On day 7 after STZ injection, rats with fasting blood glucose levels that exceeded 11.1 mM were considered diabetic. The following experiments were performed on day 28 after STZ injection.

Pharmacokinetics of Rb1 after Oral and Intravenous Administration. For oral administration, rats were fasted overnight and they received an oral dose of Rb1 (100 mg/kg). Blood samples were collected under light ether anesthesia via the orbital sinus at 0.25, 0.5, 1, 2, 4, 6, 8, 10, 12, 24, 36, 48, and 72 hours after the oral dose. For intravenous administration, Rb1 (10 mg/kg) was given to rats via the tail vein. Blood samples were collected at 0.167, 0.5, 1, 1.5, 2, 3, 4, 6, 8, 10, 12, 24, 48, and 72 hours after intravenous administration. After three or four samplings, the appropriate amount of normal saline was administered to the rats to compensate for blood loss. Plasma samples were obtained by centrifugation at 4000 rpm for 10 minutes and were stored at −80°C until analysis.

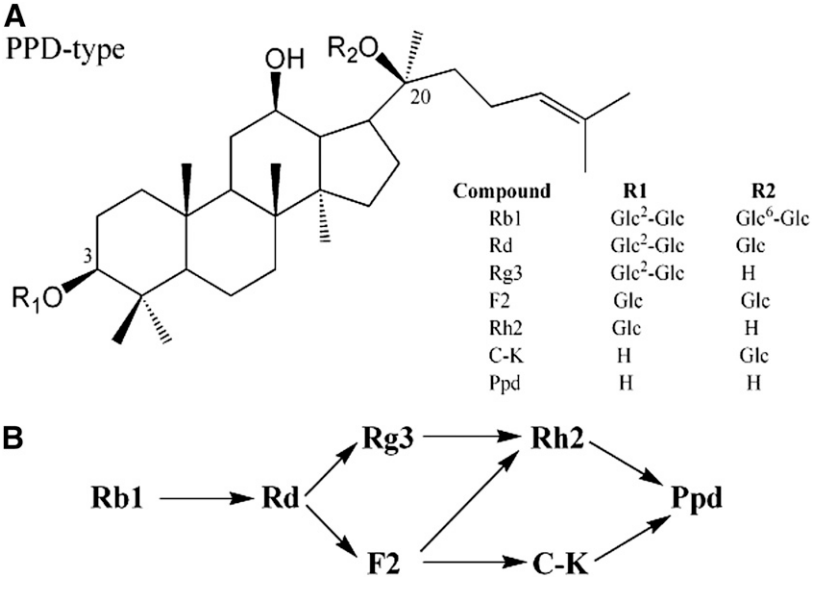

Fig. 1. (A) Structures of 20-(S)-PPD type saponins. (B) The proposed biotransformation pathway of Rb1 induced by intestinal microflora. Glc, β-D-glucose.

Portal plasma samples were also collected from another subset of experimental rats. The fasted rats were anesthetized using pentobarbital (60 mg/kg, i.p.) and portal vein cannulation was performed. Portal blood samples were collected via a cannula at 1, 2, 4, 6, and 8 hours after oral administration of Rb1 (100 mg/kg).

Rb1 Absorption via Intestinal Walls. Rb1 absorption via intestinal walls was evaluated by in situ single-pass perfusion as described previously (Yu et al., 2010). In brief, fasted rats were anesthetized using pentobarbital (60 mg/kg, i.p.), followed by the insertion of two cannulas for input and output at the two ends of the isolated jejunum (10 cm). The jejunum was returned to the abdominal cavity and the abdomen was closed. The isolated jejunal segment was preperfused with 0.9% saline solution (37°C) at 0.2 ml/min for 20 minutes, followed by Krebs-Henseleit buffer containing Rb1 (2 μg/ml) and phenol red (5 μg/ml for impermeable volume marker). After a steady state was achieved (30 minutes),

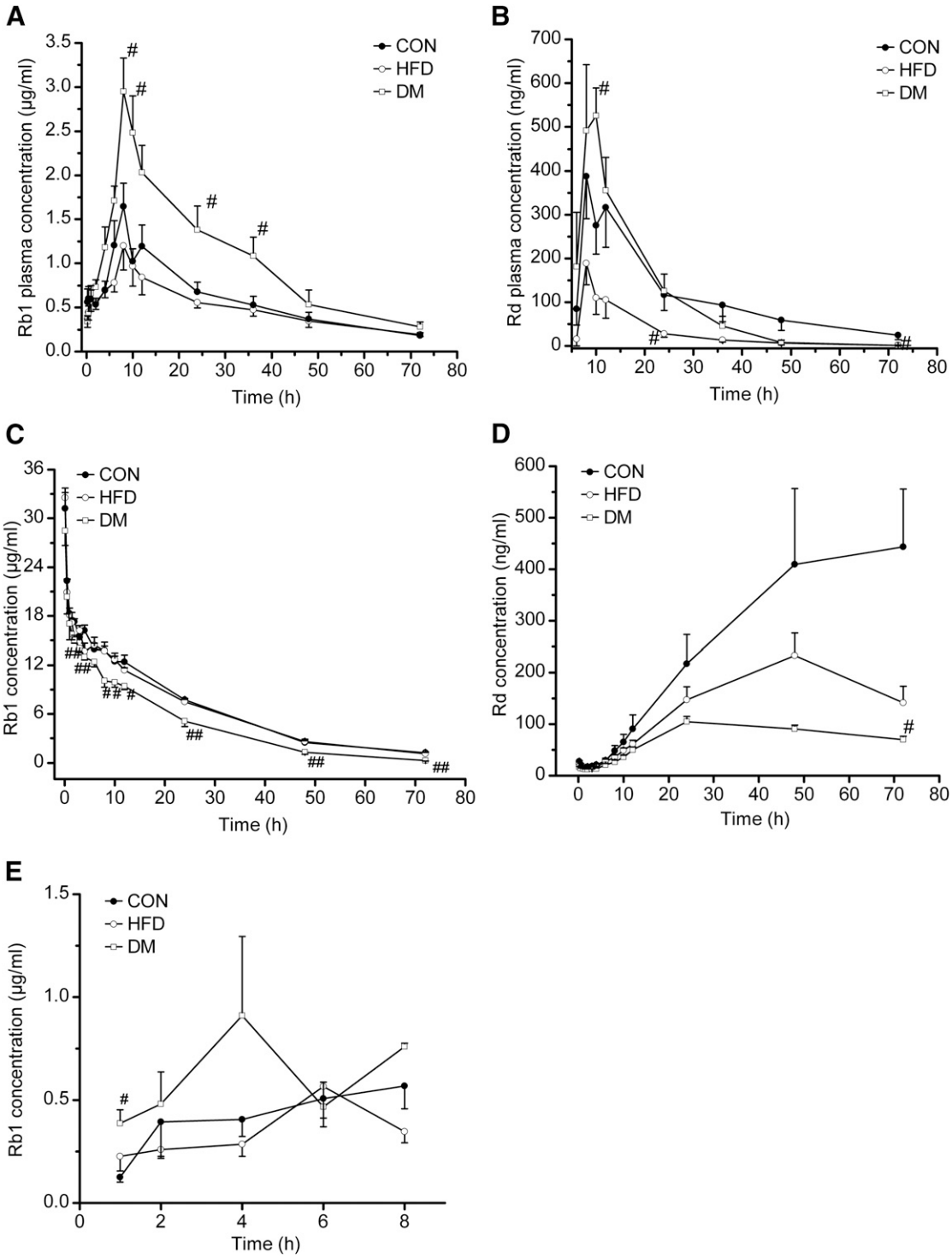

Fig. 2. (A–D) Plasma concentrations of Rb1 and its main metabolic product Rd in control, HFD-fed, and diabetic rats after administration of Rb1 orally (100 mg/kg; A and B) and intravenously (10 mg/kg; C and D). (E) Rb1 concentration in portal plasma after the oral dose (100 mg/kg). Values are expressed as means ± S.E.M. (n = 5). $^{\#}P < 0.05$; $^{\#\#}P < 0.01$ (versus control). CON, control; DM, diabetic rat.

consecutive effluent samples were collected at 15-minute intervals through the distal cannula for 120 minutes. At the end of the experiments, the animals were euthanized, perfused intestinal segments were removed, and the areas of absorption were measured. The apparent effective permeability (P_{eff}; in centimeters per minute) was calculated according to the following equation: $P_{eff} = -[Qln(C_{out}/C_{in})]/A$, where C_{out} and C_{in} indicate the output and input of Rb1 concentration, respectively. A (in square centimeters) represents the area of the perfused intestinal segment, and Q is the flow rate (0.2 ml/min).

Rb1 Excretion via Urine and Bile. For urinary excretion, experimental rats were housed individually in metabolic cages before the study. After 3-day adaption, rats received Rb1 intravenously (10 mg/kg). Urine samples were collected before dosing and at intervals of 0–6 hours, 6–12 hours, 12–18 hours, 18–24 hours, 24–36 hours, 36–48 hours, and 48–72 hours after dosing. For biliary excretion, rats were anesthetized using ether and a biliary cannula was applied via the common bile duct. After confirmation of bile flow, Rb1 (10 mg/kg) was intravenously administered to the rats, and bile samples were collected before dosing and at intervals of 0 to 1 hour, 1 to 2 hours, 2 to 3 hours, 3 to 4 hours, 4 to 6 hours, and 6 to 8 hours after dosing. Aliquots of urine and bile samples were stored at −80°C until analysis.

Rb1 Metabolism in Rat Hepatic and Intestinal Microsomes. Rat hepatic and intestinal microsomes were freshly prepared, according to a previously described method (Xie et al., 2010). Rb1 metabolism was determined by measuring the depletion of Rb1. The incubation system contained rat hepatic or intestinal microsomes (2 mg/ml) and Rb1 (0.2 μM or 0.05 μM of final concentration for hepatic or intestinal microsomes, respectively) in 0.1 M phosphate-buffered saline (pH 7.4). The mixture was preincubated for 5 minutes at 37°C, and the reaction was initiated with the addition of an NADPH-regenerating system (0.5 mM NADP, 10 mM glucose-6-phosphate, 1 U/ml glucose-6-phosphate dehydrogenase, and 5 mM $MgCl_2$). After the designated time (0, 30, 60, and 120 minutes), the reaction was terminated by adding 1 ml ice water–saturated *n*-butanol. All incubations were performed in triplicate.

Rb1 Metabolism in Rat Intestinal Content. The rats were euthanized under ether anesthesia, and the fresh contents of the small and large intestines were quickly harvested, respectively. The intestinal contents were immediately homogenized with anaerobic medium in a ratio of 1 g to 5 ml in a anaerobic environment, filtrated with gauze, and centrifuged at 825 *g* for 10 minutes at 4°C. The fresh cultured solution (supernatants) was collected in anaerobic incubation bags and was used to assess Rb1 metabolism. Rb1 (final concentration 0.65 mg/ml) was added into the above fresh cultured solution and incubated at 37°C in a shaking water bath for 0.5, 1, 2, 4, 6, 8, and 12 hours. The reaction were terminated by cooling to 4°C at the designed times. Contents of Rb1 and its metabolites in reacting systems were determined by liquid chromatography–mass spectrometry (LC-MS).

Rb1 Uptake and Transport across Cell Monolayers. Caco-2 cells and Multi-drug resistance protein 1 over-expressed MDCK cells (MDR1-MDCK) cells were cultured in Dulbecco's modified Eagle's medium (DMEM) containing 10% fetal bovine serum, 1% nonessential amino acid, 2 mM L-glutamine, 100 IU/ml penicillin, and 100 μg/ml streptomycin in a humidified atmosphere with 5% CO_2 at 37°C. Wild-type MDCK cells were also used as a control.

Rb1 bidirectional transport experiments were carried out in triplicate at 2 and 10 μM for Rb1 with or without inhibitors in Hanks' balanced salt solution (HBSS). In brief, MDR1-MDCK cells were seeded in Millicell inserts (1.2 cm diameter, 0.4 μm pore size; Millipore, Billerica, MA) and cultured. The integrity of the cell layer was monitored by measurement of transepithelial electrical resistance (TEER) with Millicell-ERS equipment (Millipore). Only the monolayer with a TEER value of more than 300 $\Omega \cdot cm^2$ was used. Rb1 was loaded onto either apical or basolateral compartments with or without inhibitors. Samples were taken at 2 hours from the opposite compartment. The apparent permeability coefficient was calculated as follows: $P_{app} = dQ/AC_0dt$, where dQ/dt is the rate of permeability (in nanomoles per second), A is the surface area of the insert (in square centimeters), and C_0 is the initial concentration.

Studies on the effect of experimental rat serum on Caco-2 monolayer permeability and Rb1 transport across the Caco-2 monolayer were conducted. Transport studies were initiated the same as described above, except that the medium was replaced with DMEM containing 10% rat serum 8 days before the study to simulate in vivo conditions. Serum was collected from age-matched control, HFD-fed, and diabetic rats and was inactivated for 30 minutes at 56°C. Caco-2 monolayer permeability was evaluated by measuring FD-4 and FLU transport (apical to basolateral) across the monolayer. Meanwhile, Rb1 transport was also performed under the same condition.

Effects of transporter inhibitors on Rb1 uptake by Caco-2 cells were also measured. Caco-2 cells cultured in 24-well plates were incubated with Rb1 (50 μM) with or without inhibitors in HBSS. Cellular uptake was terminated by removing the incubation solution and rinsing with ice-cold HBSS three times. Purified water was added to each incubated well, frozen, and melted repeatedly three times and then ultrasonically treated to break down cells. Rb1 was extracted with water-saturated *n*-butanol. Cellular Rb1 content was normalized to protein contents, which were determined using the Bradford method.

Determination of Ginsenosides by LC-MS. A validated LC-MS method was employed to analyze ginsenoside content, according to a previously described method with minor modifications (Liu et al., 2013). Briefly, ginsenosides were extracted with water-saturated *n*-butanol from biologic samples, including plasma, urine, bile, intestinal perfusate, microsomes, and cell culture medium. Separation was performed at a flow rate of 0.2 ml/min with a Waters Symmetry C_{18} column (5.0 μm, 2.1 mm × 150 mm). The mobile phase was composed of a mixture of NH_4Cl (0.15 mM) in water (A) and acetonitrile (B). The gradient conditions were as follows: 0–3 minutes at 25% B, 3–5 minutes at 25%→50% B, 5–14 minutes at 50% B, 14–18 minutes at 50%→65% B, 18–28 minutes at 65% B, 28–29 minutes at 65%→25%, and 29–32 minutes at 25%. Analysis in the mass spectrometer with an electrospray ionization probe was operated in the selected ion monitoring mode with the following mass-to-charge ratios: $[M + Cl]^{2-}$ 589.25 for Rb1, $[M + Cl]^-$ 981.45 for Rd, $[M + Cl]^-$ 819.4 for Rg3 and F2, $[M + Cl]^-$ 657.3 for Rh2 and C-K, $[M + Cl]^-$ 495.25 for PPD, and $[M + Cl]^-$ 815.35 for digoxin (internal standard). The injection volume was 5 μl. Calibration curves constructed for the analytes (10–1000 ng/ml) showed good linearity ($r^2 > 0.999$).

Statistical Analysis. Pharmacokinetic parameters were calculated by noncompartmental analysis (Phoenix WinNonlin 6.1; Pharsight, St. Louis, MO). The AUC was calculated by the trapezoidal rule with extrapolation to infinity. The oral clearance was calculated as dose/AUC. The terminal elimination constant was obtained from the least-squares linear regression slope of ln-concentration versus time, and terminal elimination half-life was calculated as 0.693/*k*. All data are expressed as means ± S.E.M. Statistical differences among groups were evaluated using one-way analysis of variance followed by

TABLE 1

Pharmacokinetic parameters of Rb1 and Rd in control, HFD-fed, and diabetic rats

Values are expressed as means ± S.E.M. (n = 4 to 5).

Parameter	Control Rats	HFD-Fed Rats	Diabetic Rats
Rb1 (100 mg/kg p.o.)			
Rb1			
$AUC_{0-\infty}$ (μg/ml·h)	42.47 ± 7.26	35.61 ± 5.24	75.63 ± 12.10[a]
C_{max} (μg/ml)	1.73 ± 0.25	1.20 ± 0.28	3.09 ± 0.34[a]
t_{max} (h)	8.80 ± 0.80	8.00	8.40 ± 0.40
$t_{1/2}$ (h)	24.00 ± 1.10	25.03 ± 1.66	20.08 ± 1.42
MRT (h)	25.03 ± 0.54	27.01 ± 1.09	24.46 ± 0.94
F (%)	0.90	0.78	2.25
CL (l/h per kilogram)	2.38 ± 0.49	2.56 ± 0.40	1.37 ± 0.28
Rd			
$AUC_{0-\infty}$ (μg/ml·h)	7.59 ± 2.25	2.40 ± 0.53	6.85 ± 0.88
C_{max} (μg/ml)	0.45 ± 0.08	0.21 ± 0.05[a]	0.65 ± 0.07
t_{max} (h)	8.80 ± 0.80	8.00	8.80 ± 0.49
$t_{1/2}$ (h)	16.78 ± 3.24	12.34 ± 3.21	9.27 ± 1.91
MRT (h)	22.31 ± 2.71	18.18 ± 1.53	15.53 ± 1.71
Rb1 (10 mg/kg i.v.)			
Rb1			
$AUC_{0-\infty}$ (μg/ml·h)	472.3 ± 15.2	458.1 ± 22.0	335.6 ± 22.1[b]
V_d (ml/kg)	520.5 ± 15.9	523.9 ± 20.0	479.2 ± 17.5
$t_{1/2}$ (h)	18.19 ± 0.55	17.64 ± 1.00	11.26 ± 0.70[b]
MRT (h)	19.42 ± 0.32	19.50 ± 0.61	15.80 ± 0.93[b]
CL (ml/h per kilogram)	19.88 ± 0.67	20.80 ± 1.31	29.86 ± 2.26[b]
Rd			
AUC_{0-72h} (μg/ml·h)	20.05 ± 6.14	10.67 ± 1.19	5.08 ± 0.35[a]

CL, clearance; F, bioavailability; MRT, mean residence time; $t_{1/2}$, terminal elimination half-life.

[a] $P < 0.05$ versus control.

[b] $P < 0.01$ versus control.

a Student–Newman–Keuls post hoc test. A P value of less than 0.05 was considered statistically significant.

Results

Pharmacokinetic Profiles of Rb1 after Oral and Intravenous Administration. Plasma concentrations of Rb1 and Rd in control, HFD-fed, and diabetic rats after oral administration of Rb1 were measured (Fig. 2, A and B) and main pharmacokinetic parameters were estimated (Table 1). The results showed that diabetes significantly enhanced the systemic exposure of Rb1, evidenced by significantly higher C_{max} and $AUC_{0-\infty}$. A long half-life of Rb1 was estimated in each group, whereas diabetic rats showed a relatively shorter terminal elimination half-life. Collectively, oral bioavailability of Rb1 in diabetic rats (Table 1) was significantly increased by 2.50- and 2.88-fold in control and HFD-fed rats, respectively. It was also found that diabetes showed a trend to increase Rd concentration. A significant increase was observed 10 hours after dosing; however, the C_{max} and $AUC_{0-\infty}$ values of Rd were slightly altered by diabetes. Feeding with a HFD decreased plasma exposure of Rb1 and Rd in diabetic rats compared with control rats, and a significant decrease in C_{max} values of Rd was obtained.

Pharmacokinetic profiles of Rb1 in rats were also measured after intravenous administration of Rb1 (Fig. 2C). Diabetes significantly decreased the plasma concentration of Rb1 after the intravenous dose, accompanied by a significant decrease in $AUC_{0-\infty}$ values and an increase in systematic Rb1 clearance. A significant decrease in exposure of Rd was also observed in diabetic rats (Fig. 2D; Table 1). These results indicated that the increased exposure of Rb1 after oral administration of Rb1 in diabetic rats cannot be attributed to alterations in systematic clearance.

To exclude hepatic contribution to the alteration of systemic exposure after oral administration, plasma concentrations of Rb1 in the portal vein were evaluated (Fig. 2E). Consistent with our expectations, the portal Rb1 concentrations in diabetic rats were higher than those in control rats and HFD-fed rats, leading to marked increases in AUC_{0-8h} of Rb1 (3.79 ± 0.88 μg·h/ml, 2.72 ± 0.85 μg·h/ml, and 2.58 ± 0.54 μg·h/ml in diabetic, control, and HFD-fed rats, respectively), implying that Rb1 absorption was enhanced under diabetic conditions.

Rb1 Absorption via Intestinal Walls. Accumulative Rb1 absorption was assessed using in situ intestinal perfusion (Fig. 3A) and corresponding P_{eff} values (Fig. 3B) were estimated. Results showed that accumulative Rb1 absorption was significantly enhanced by diabetes. Significant increases were observed in P_{eff} values of Rb1 at 45 minutes and 105 minutes after perfusion. These results implied that diabetes enhanced Rb1 absorption via intestinal walls, which was in line with in vivo findings.

Rb1 Biliary and Urinary Excretion Studies. In most cases, ginsenosides are supposed to have rapid and extensive biliary excretion (43%–100% of intravenous dose), whereas Rb1 is relatively lower (approximately 10%) (Liu et al., 2009). However, in this study, the contribution of biliary excretion to the overall Rb1 elimination was very limited (less than 1% of intravenous dose), although it is of interest that accumulative biliary excretion of Rb1 and Rd in diabetic rats is significantly lower than control rats (Fig. 3, C and D).

By contrast, approximately 87.8% of intravenously administrated Rb1 was excreted via urine in diabetic rats, which is markedly higher than that of control rats and HFD-fed rats (50.7% and 43.9%,

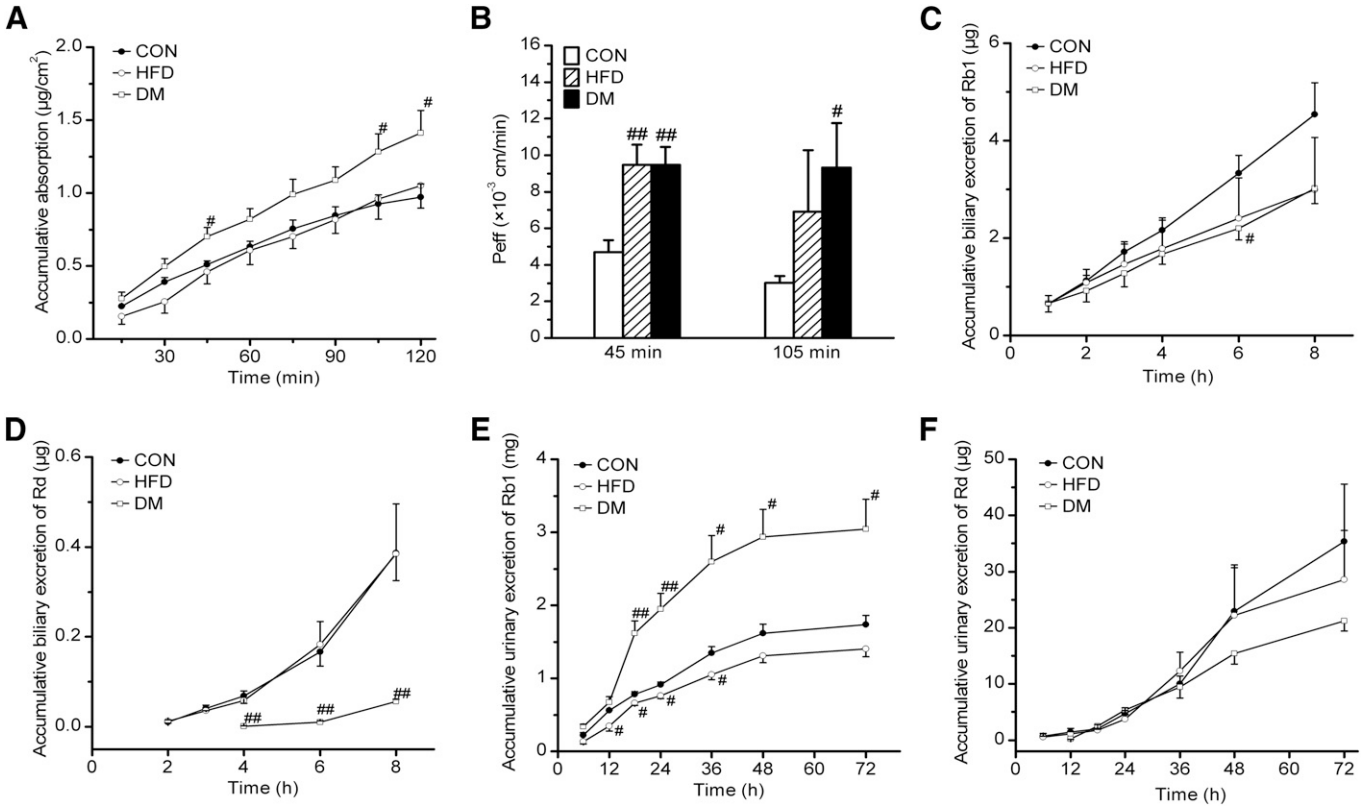

Fig. 3. (A and B) Accumulative absorption of Rb1 (A) and corresponding P_{eff} values (B) were measured using in situ, single-pass perfusion of the jejunum in experimental rats. (C–F) Biliary (C and D) and urinary (E and F) excretion of Rb1 and Rd after intravenous Rb1 administration (10 mg/kg). Values are expressed as means ± S.E.M. (n = 5). $^{\#}P < 0.05$; $^{\#\#}P < 0.01$ (versus control). CON, control; DM, diabetic rat.

respectively; Fig. 3E). Significant increases in Rb1 excretion via urine may largely contribute to the low systemic exposure of Rb1 after intravenous administration under diabetic status. Urinary excretion of Rd via urine in diabetic rats showed a trend to decrease (Fig. 3F), but no significance was observed.

Metabolism of Rb1 by Microsomes and Intestinal Microflora. To further elucidate whether metabolic enzymes contributed to the change in Rb1 pharmacokinetic profile in diabetic rats, Rb1 depletion via both hepatic and intestinal microsomes was investigated. In contrast with our expectations, Rb1 metabolism by hepatic and intestinal microsomes was extremely weak, although diabetic rats showed greater Rb1 depletion (Fig. 4, A and B), indicating that Rb1 metabolism by microsomes is not a dominant pathway of Rb1 elimination.

It was confirmed that deglycosylation of ginsenosides was the major biotransformation pathway after oral dosing. To gain more insight into the alterations of Rb1 biotransformation by diabetes, formation of Rb1 metabolites incubated with intestinal contents from control, HFD-fed, and diabetic rats was identified.

C-K was the main metabolite of Rb1when Rb1 incubated with the intestinal microflora of the large intestine, which was in agreement with a previous report (Tawab et al., 2003). However, the generation of C-K was extremely reduced in diabetic group (Fig. 4C), suggesting that deglycosylation of Rb1 was inhibited under diabetic conditions.

Generation of Rd in the reaction system varied with time processes. Rd initially reached a high level and then decreased steadily in the control and HFD-fed groups (Fig. 4D), indicating that Rd was produced rapidly and then further decomposed to other secondary metabolites (e.g., F2 and C-K). A similar profile was observed in the generation of F2 (Fig. 4E). By contrast, the initial product of Rd in diabetic group was much lower than control group. Then it increased and

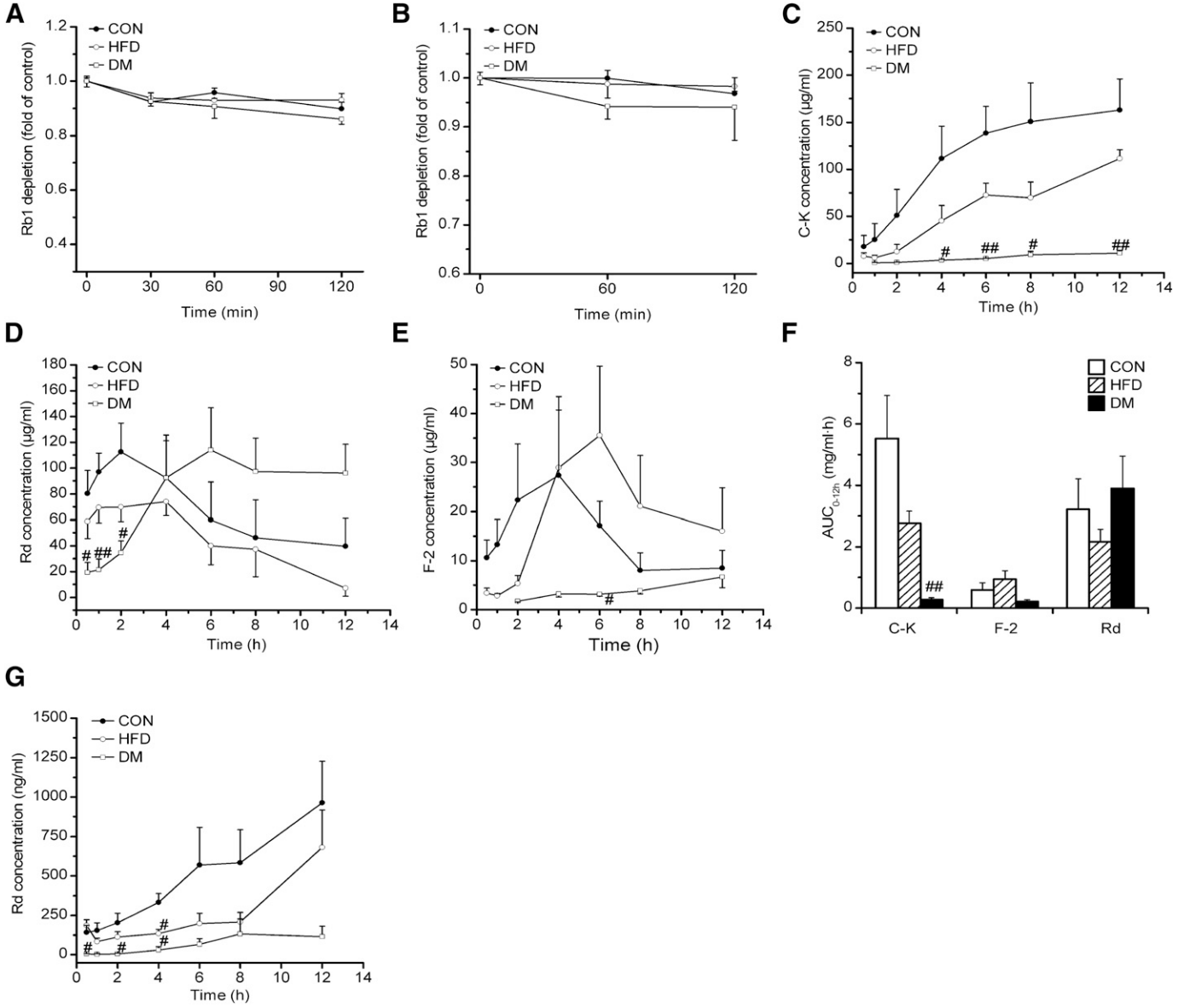

Fig. 4. (A and B) Metabolism of Rb1 in hepatic (A) and intestinal (B) microsomes from control, HFD-fed, and diabetic rats in vitro. Depletion of Rb1 (200 nM) in hepatic microsomes was measured with incubation times of 0, 30, 60, and 120 minutes, whereas depletion of Rb1 (50 nM) in intestinal microsomes was measured with incubation times of 0, 60, and 120 minutes. (C–F) Concentration-time profiles of C-K (C), Rd (D), and F2 (E) and corresponding AUC_{0-12h} values (F) metabolized by large intestinal microflora from control, HFD-fed, and diabetic rats. (G) Concentration-time profile of Rd metabolized by contents of the small intestine. Values are expressed as means ± S.E.M. ($n = 4$). $^{\#}P < 0.05$; $^{\#\#}P < 0.01$ (versus control). CON, control; DM, diabetic rat.

remained stable high without a further decrease (Fig. 4D), indicating that formation of Rd under diabetic status was inhibited and secondary deglycosylation was abrogated (Fig. 4, C and E). As a result, Rd accumulation during incubation in diabetic group led to higher AUC_{0-12h} values of Rd compared with controls (Fig. 4F), and it further lead to extremely low generation of C-K and F2 (Fig. 4, C, E, and F).

When incubated with contents of the small intestine (Fig. 4G), Rb1 was mainly degraded to Rd by stripping one sugar moiety. Similarly, the generation of Rd in diabetic group was much lower than those in the control and HFD-fed groups. These findings demonstrate that considerable degradation of Rb1 in the gastrointestinal tract of normal rats was drastically attenuated by diabetes, which partly remained in HFD-fed rats.

Rb1 Uptake and Transport across the Cell Monolayer. To identify whether increased Rb1 absorption was associated with transporters, the effects of P-gp and organic anion-transporting polypeptide (Oatp) inhibitors on Rb1 transport were investigated. Fig. 5A shows Rb1 transport across monolayers of MDCK and P-gp overexpressed MDR1-MDCK cells. Rb1 efflux ratios were less than 2 and P-gp inhibitors (verapamil and cyclosporine A) did not affect the efflux ratio, indicating that Rb1 was not a substrate of P-gp. Data from Rb1 uptake showed that neither Oatp 1a4 inhibitors (bromosulfalein and rifampicin) nor Oatp 1a5 inhibitors (naringin and levofloxacin) exhibited an appreciable effect on Rb1 uptake by Caco-2 cells (Fig. 5B).

It is known that gut permeability is one of the determining factors for drug transport. Thus, transport studies of FD4 and FLU across Caco-2 were performed to evaluate the alteration of paracellular permeability under diabetic conditions. The Caco-2 monolayer was pretreated with DMEM supplemented with 10% rat serum (for all three groups) for 8 days to simulate the internal environment. TEER measurements of the cell monolayer showed that incubation with diabetic rat serum remarkably decreased TEER (508 $\pm$ 14.1 $\Omega \cdot cm^2$ and 725 $\pm$ 15.9 $\Omega \cdot cm^2$ for diabetic rats versus control rats; $P < 0.01$). Furthermore, incubation with 10% diabetic rat serum significantly increased transport of FD-4 and FLU across the Caco-2 monolayer in the A to B direction (Fig. 5C) which indicated that paracellular permeability of the monolayer was increased under diabetic conditions. Similarly, incubation with 10% diabetic rat serum significantly increased Rb1 transport across Caco-2 monolayer in the apical to basolateral and basolateral to apical directions (Fig. 5D); the extent of the increase in the apical to basolateral direction was larger than that in the basolateral to apical direction.

Discussion

Previous reports mainly focused on the antidiabetic actions of ginsenosides (Park et al., 2002; Park et al., 2008; Shang et al., 2008) as well as their pharmacokinetic properties under normal conditions. However, very little was known about pharmacokinetic behaviors of ginsenosides under diabetic conditions. The main finding of this study was that diabetes significantly increased Rb1 systemic exposures after oral administration. Although ginsenosides were considered to be of poor absorption, diabetes increased the exposure level of Rb1 after oral administration, which is beneficial to Rb1 treatment as an antidiabetic remedy. Meanwhile, diabetes decreased systemic Rb1 exposure after intravenous administration and increased portal Rb1 concentration, implying that increased exposure of Rb1 after oral administration under diabetic conditions was at least partly attributable to alterations in intestinal systems.

Data from in situ intestinal perfusion studies demonstrated that enhancement of Rb1 absorption was partly attributed to Rb1 transport across intestinal walls. In previous studies, diabetes downregulated intestinal P-gp function and Rh2 and C-K were identified as the substrate of P-gp (Liu et al., 2009; Yang et al., 2011, 2012); however, these findings were controversial, implying that increased Rb1 absorption may be associated with downregulation of intestinal P-gp

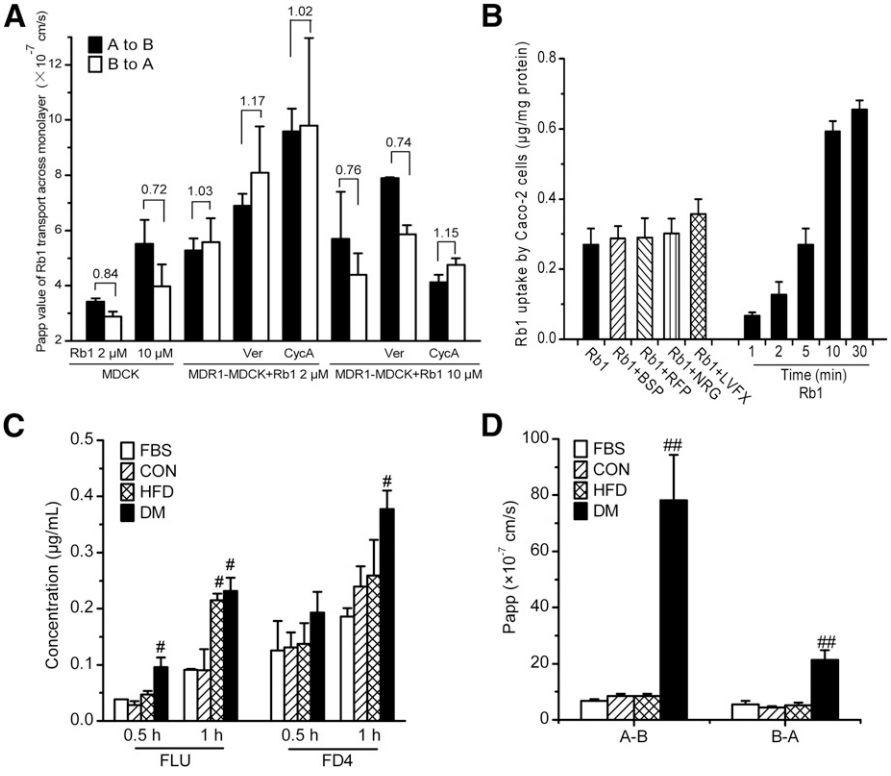

Fig. 5. (A) P_{app} values of Rb1 (2 μM and 10 μM) transport across monolayers of MDCK and MDR1-MDCK cells with and without P-gp inhibitors (50 μM verapamil or 20 μM cyclosporine A). Efflux ratios are shown over the bars. (B) cellular uptake of Rb1 at 50 μM by Caco-2 cells with and without Oatp inhibitors, namely bromosulfalein (100 μM), rifampicin (20 μM), naringin (1 mM), and levofloxacin (500 μM) for 5 minutes. (C) Transport of FD4 (1 mg/ml) and FLU (0.1 mg/mL) from the apical to basal (A→B) direction was measured to evaluate the permeability of the Caco-2 monolayer cultured with 10% rat serum. (D) Rb1 (10 μM) transport across the Caco-2 monolayer cultured with 10% rat serum from both the A→B and B→A direction. Caco-2 cells were pretreated with 10% rat serum for 8 days. Values are expressed as means $\pm$ S.E.M. ($n = 3$–5). $^{\#}P < 0.05$; $^{\#\#}P < 0.01$ (versus control). BSP, bromosulfalein; CON, control; CycA, cyclosporine A; DM, diabetic rat; LVFX, levofloxacin; NRG, naringin; RFP, rifampicin; Ver, verapamil.

under diabetic conditions. Unfortunately, our data showed that Rb1 transport across the MDR1-MDCK monolayer was not regulated by P-gp. In addition, Rb1 seemed not to be a substrate of Oatps. Several reports showed that some oxygenated metabolites of Rb1, Rg3, and Rh2 mediated by P450 enzymes had been identified (Qian et al., 2005a, b, 2006). Our results showed that its contribution to Rb1 depletion can be negligible due to the extremely poor capacity of Rb1 metabolism in hepatic and intestinal microsomes. Similar results were found in protopanaxatriol-type ginsenosides (Hao et al., 2010). Compared with some deglycosylated metabolites such as Rh1 and Rf, Re and Rb1 were not easily metabolized by CYP3A4, implying that efficiency of oxygenation was reduced due to sugar moieties at the C-20 site. Taken together, Rb1 disposition may not be markedly regulated by transporters or P450 enzymes.

Intestinal microflora–mediated deglycosylation is considered the main metabolic pathway of ginsenosides (Qian et al., 2006). Under normal status, Rb1 was metabolized to Rd, which was further metabolized to F2 and C-K. Our results showed that further deglycosylation of Rd was drastically abrogated under diabetic conditions, leading to the accumulation of Rb1 and Rd in the intestinal lumen, which may directly contribute to the increased exposure of Rb1 and Rd (Fig. 2, A and B) and decreased exposure of F-2 and C-K (data not shown) in vivo. Deglycosylation of Rb1 in HFD-fed rats was less inhibited compared with diabetic rats, which was reflected by higher F2 accumulation and C-K formation (Fig. 4, C, E, and F). In addition, Rd may be the only detectable metabolite after intravenous administration of Rb1, implying that deglycosylation of Rb1 also occurred in vivo. However, AUC_{0-72h} of Rd in control rats only accounted for approximately 0.06% of the i.v. dose, whereas that of diabetic rats was much lower.

On one hand, the major factor limiting intestinal absorption of ginsenosides is poor membrane permeability, which was mainly due to high molecular weight and hydrogen bond counts (Liu et al., 2009). On the other hand, the increased paracellular permeability of the intestinal epithelium under diabetic conditions may benefit Rb1 absorption. The Caco-2 monolayer was precultured with rat serum to simulate the intestinal environment. FLU and FD-4 are used as markers of transepithelial transport. The results demonstrated that culture with diabetic serum significantly decreased TEER and increased FD-4, FLU, and Rb1 transport across the Caco-2 monolayer, implying that enhancement of Rb1 intestinal absorption by diabetes partly came from the impairment of intestinal integrity. Occludin and zonula occludens-1 are known as important tight conjunction proteins in integrity function. Whether Rb1 absorption is associated with the distribution of occludin and zonula occludens-1 is an area for future exploration (Cani et al., 2008).

Our study also showed that urinary excretion of Rb1 (approximately 87.8% of dose) in diabetic rats was significantly higher that that of control rats (50.7%) and HFD-fed rats (43.9%), implying that increased urinary excretion of Rb1 may result in lower plasma exposure of Rb1 after intravenous Rb1 administration. Increased urine volume is proposed to be an important factor in the higher renal clearance of Rb1. Hyperfiltration is the marked feature of diabetic nephropathy, which may also lead to high renal clearance of Rb1. Apart from this, although Rb1 was proven not to be a substrate of P-gp and Oatp, other transporters may have the potential to mediate Rb1 transport (e.g., sodium-dependent glucose transporter 1 (SGLT1); Xiong et al., 2009). Therefore, the effect of diabetic nephropathy and possible regulator SGLT1/2 in renal tubules on Rb1 elimination should be considered in the further studies. possible regulator SGLT1/SGLT2 in renal tubules.

In addition to normal controls, HFD-fed rats were set as the other control group due to high-fat diet induced metabolic syndrome including hyperlipidemia as well as insulin resistance (Liu et al., 2014). HFD treatment exhibited a trend to decrease the oral exposure of Rb1 and Rd compared with control rats, which was opposite of diabetic rats (Fig. 2, A and B; Table 1). HFD-fed rats showed similar $AUC_{0-\infty}$ and clearance as control rats after intravenous administration of Rb1 (Table 1). The portal concentration and intestinal absorption of Rb1 was mildly lower than in control rats (Figs. 2E and 3A), which may partly explain the decreased oral Rb1 exposure. In vitro, HFD serum treatment showed a trend to increase the permeability of the Caco-2 monolayer but failed to increase Rb1 transport (Fig. 5, C and D). This indicated that the paracellular pathway did not play a key role in the alteration of Rb1 exposure in HFD-fed rats. Further investigations are required.

In conclusion, diabetes significantly increased plasma exposure of Rb1 after oral administration. The combined effect of increased Rb1 intestinal absorption and inhibited Rb1 deglycosylation may play an important role. This study provides an important reference for clinical use of ginseng.

Authorship Contributions

Participated in research design: C. Liu, L. Liu, X. Liu.
Conducted experiments: C. Liu, Hu, M. Zhang, J. Zhang, F. Li, Y. Li, P. Xu.
Performed data analysis: C. Liu, Guo, Zhong, Chen, J. Li, L. Liu.
Wrote or contributed to the writing of the manuscript: C. Liu, X. Liu.

References

Attele AS, Wu JA, and Yuan CS (1999) Ginseng pharmacology: multiple constituents and multiple actions. *Biochem Pharmacol* **58**:1685–1693.

Attele AS, Zhou YP, Xie JT, Wu JA, Zhang L, Dey L, Pugh W, Rue PA, Polonsky KS, and Yuan CS (2002) Antidiabetic effects of *Panax ginseng* berry extract and the identification of an effective component. *Diabetes* **51**:1851–1858.

Bosi E, Molteni L, Radaelli MG, Folini L, Fermo I, Bazzigaluppi E, Piemonti L, Pastore MR, and Paroni R (2006) Increased intestinal permeability precedes clinical onset of type 1 diabetes. *Diabetologia* **49**:2824–2827.

Cani PD, Bibiloni R, Knauf C, Waget A, Neyrinck AM, Delzenne NM, and Burcelin R (2008) Changes in gut microbiota control metabolic endotoxemia-induced inflammation in high-fat diet-induced obesity and diabetes in mice. *Diabetes* **57**:1470–1481.

Chen GM, Hu N, Liu L, Xie SS, Wang P, Li J, Xie L, Wang GJ, and Liu XD (2011) Pharmacokinetics of verapamil in diabetic rats induced by combination of high-fat diet and streptozotocin injection. *Xenobiotica* **41**:494–500.

Dostalek M, Akhlaghi F, and Puzanovova M (2012) Effect of diabetes mellitus on pharmacokinetic and pharmacodynamic properties of drugs. *Clin Pharmacokinet* **51**:481–499.

Hao H, Lai L, Zheng C, Wang Q, Yu G, Zhou X, Wu L, Gong P, and Wang G (2010) Microsomal cytochrome p450-mediated metabolism of protopanaxatriol ginsenosides: metabolite profile, reaction phenotyping, and structure-metabolism relationship. *Drug Metab Dispos* **38**: 1731–1739.

Hasegawa H, Sung JH, Matsumiya S, and Uchiyama M (1996) Main ginseng saponin metabolites formed by intestinal bacteria. *Planta Med* **62**:453–457.

Hu N, Xie S, Liu L, Wang X, Pan X, Chen G, Zhang L, Liu H, Liu X, and Liu X, et al. (2011) Opposite effect of diabetes mellitus induced by streptozotocin on oral and intravenous pharmacokinetics of verapamil in rats. *Drug Metab Dispos* **39**:419–425.

Kim YC, Lee JH, Kim SH, and Lee MG (2005) Effect of CYP3A1(23) induction on clarithromycin pharmacokinetics in rats with diabetes mellitus. *Antimicrob Agents Chemother* **49**:2528–2532.

Kimura M, Waki I, Chujo T, Kikuchi T, Hiyama C, Yamazaki K, and Tanaka O (1981) Effects of hypoglycemic components in ginseng radix on blood insulin level in alloxan diabetic mice and on insulin release from perfused rat pancreas. *J Pharmacobiodyn* **4**:410–417.

Lee JH and Lee MG (2008) Telithromycin pharmacokinetics in rat model of diabetes mellitus induced by alloxan or streptozotocin. *Pharm Res* **25**:1915–1924.

Liu C, Hu MY, Zhang M, Li F, Li J, Zhang J, Li Y, Guo HF, Xu P, and Liu L, et al. (2014) Association of GLP-1 secretion with anti-hyperlipidemic effect of ginsenosides in high-fat diet fed rats. *Metabolism* **63**:1342–1351.

Liu C, Zhang M, Hu MY, Guo HF, Li J, Yu YL, Jin S, Wang XT, Liu L, and Liu XD (2013) Increased glucagon-like peptide-1 secretion may be involved in antidiabetic effects of ginsenosides. *J Endocrinol* **217**:185–196.

Liu H, Liu L, Li J, Mei D, Duan R, Hu N, Guo H, Zhong Z, and Liu X (2012) Combined contributions of impaired hepatic CYP2C11 and intestinal breast cancer resistance protein activities and expression to increased oral glibenclamide exposure in rats with streptozotocin-induced diabetes mellitus. *Drug Metab Dispos* **40**:1104–1112.

Liu H, Yang J, Du F, Gao X, Ma X, Huang Y, Xu F, Niu W, Wang F, and Mao Y, et al. (2009) Absorption and disposition of ginsenosides after oral administration of Panax notoginseng extract to rats. *Drug Metab Dispos* **37**:2290–2298.

Odani T, Tanizawa H, and Takino Y (1983a) Studies on the absorption, distribution, excretion and metabolism of ginseng saponins. II. The absorption, distribution and excretion of ginsenoside Rg1 in the rat. *Chem Pharm Bull (Tokyo)* **31**:292–298.

Odani T, Tanizawa H, and Takino Y (1983b) Studies on the absorption, distribution, excretion and metabolism of ginseng saponins. III. The absorption, distribution and excretion of ginsenoside Rb1 in the rat. *Chem Pharm Bull (Tokyo)* **31**:1059–1066.

Park KH, Shin HJ, Song YB, Hyun HC, Cho HJ, Ham HS, Yoo YB, Ko YC, Jun WT, and Park HJ (2002) Possible role of ginsenoside Rb1 on regulation of rat liver triglycerides. *Biol Pharm Bull* **25**:457–460.

Park MW, Ha J, and Chung SH (2008) 20(S)-ginsenoside Rg3 enhances glucose-stimulated insulin secretion and activates AMPK. *Biol Pharm Bull* **31**:748–751.

Qian T, Cai Z, Wong RN, and Jiang ZH (2005a) Liquid chromatography/mass spectrometric analysis of rat samples for in vivo metabolism and pharmacokinetic studies of ginsenoside Rh2. *Rapid Commun Mass Spectrom* **19**:3549–3554.

Qian T, Cai Z, Wong RN, Mak NK, and Jiang ZH (2005b) In vivo rat metabolism and pharmacokinetic studies of ginsenoside Rg3. *J Chromatogr B Analyt Technol Biomed Life Sci* **816**: 223–232.

Qian T, Jiang ZH, and Cai Z (2006) High-performance liquid chromatography coupled with tandem mass spectrometry applied for metabolic study of ginsenoside Rb1 on rat. *Anal Biochem* **352**:87–96.

Sapone A, de Magistris L, Pietzak M, Clemente MG, Tripathi A, Cucca F, Lampis R, Kryszak D, Cartenì M, and Generoso M, et al. (2006) Zonulin upregulation is associated with increased gut permeability in subjects with type 1 diabetes and their relatives. *Diabetes* **55**:1443–1449.

Shang W, Yang Y, Zhou L, Jiang B, Jin H, and Chen M (2008) Ginsenoside Rb1 stimulates glucose uptake through insulin-like signaling pathway in 3T3-L1 adipocytes. *J Endocrinol* **198**: 561–569.

Sotaniemi EA, Haapakoski E, and Rautio A (1995) Ginseng therapy in non-insulin-dependent diabetic patients. *Diabetes Care* **18**:1373–1375.

Tawab MA, Bahr U, Karas M, Wurglics M, and Schubert-Zsilavecz M (2003) Degradation of ginsenosides in humans after oral administration. *Drug Metab Dispos* **31**:1065–1071.

Vuksan V, Sievenpiper JL, Koo VY, Francis T, Beljan-Zdravkovic U, Xu Z, and Vidgen E (2000) American ginseng (*Panax quinquefolius L*) reduces postprandial glycemia in nondiabetic subjects and subjects with type 2 diabetes mellitus. *Arch Intern Med* **160**:1009–1013.

Xie JT, Mchendale S, and Yuan CS (2005) Ginseng and diabetes. *Am J Chin Med* **33**:397–404.

Xie SS, Hu N, Jing XY, Liu XD, Xie L, Wang GJ, and Liu CH (2010) Effect of Huang-Lian-Jie-Du-Decoction on pharmacokinetics of verapamil in rats. *J Pharm Pharmacol* **62**: 440–447.

Xiong J, Sun M, Guo J, Huang L, Wang S, Meng B, and Ping Q (2009) Active absorption of ginsenoside Rg1 in vitro and in vivo: the role of sodium-dependent glucose co-transporter 1. *J Pharm Pharmacol* **61**:381–386.

Yang Z, Gao S, Wang J, Yin T, Teng Y, Wu B, You M, Jiang Z, and Hu M (2011) Enhancement of oral bioavailability of 20(S)-ginsenoside Rh2 through improved understanding of its absorption and efflux mechanisms. *Drug Metab Dispos* **39**:1866–1872.

Yang Z, Wang JR, Niu T, Gao S, Yin T, You M, Jiang ZH, and Hu M (2012) Inhibition of P-glycoprotein leads to improved oral bioavailability of compound K, an anticancer metabolite of red ginseng extract produced by gut microflora. *Drug Metab Dispos* **40**:1538–1544.

Yu S, Yu Y, Liu L, Wang X, Lu S, Liang Y, Liu X, Xie L, and Wang G (2010) Increased plasma exposures of five protoberberine alkaloids from Coptidis Rhizoma in streptozotocin-induced diabetic rats: is P-GP involved? *Planta Med* **76**:876–881.

Address correspondence to: Dr. Xiaodong Liu or Dr. Li Liu, Center of Drug Metabolism and Pharmacokinetics, China Pharmaceutical University, No. 24 Tongjiaxiang, Nanjing 210009, China. E-mail: xdliu@cpu.edu.cn or liulee@yeah.net